[AMERICAN JOURNAL OF SCIENCE, VOL. 299, DECEMBER, 1999, P. 805–827]

A 400 MILLION YEAR CARBON ISOTOPE RECORD OF PEDOGENIC CARBONATE: IMPLICATIONS FOR PALEOATMOSPHERIC CARBON DIOXIDE

DOUGLAS D. EKART,* THURE E. CERLING,* ISABEL P. MONTAÑEZ,** AND NEIL J. TABOR**

ABSTRACT. A 400 my record of atmospheric carbon dioxide levels has been estimated by applying a CO_2 paleobarometer to a database of 758 analyses of paleosol (fossil soil) carbonates. This database is a compilation of new data and previously published values from the literature. Many new analyses of Mesozoic paleosols are reported, an era poorly represented in the literature. Results indicate that large fluctuations in atmospheric carbon dioxide levels have occurred over the study interval, ranging from the current level up to ten times the current level. Declining pCO_2 levels through the middle Paleozoic culminate in low levels in the Early Permian. An abrupt increase in pCO_2 in the Early Permian is followed by a decrease prior to the Permo-Triassic boundary. Carbon dioxide levels increase through the Triassic to approx 3000 ppmV, a level maintained through the Jurassic period. Levels lowered through the Cretaceous, dropping to less than 1000 ppmV prior to the Cretaceous-Tertiary boundary. Relatively low levels persisted throughout the Cenozoic, with some evidence of higher levels in the Eocene and Oligocene.

INTRODUCTION

The history of atmospheric carbon dioxide is of both academic and practical interest. During the last two centuries, anthropogenic emissions have significantly increased atmospheric CO_2 levels from a pre-industrial level of approx 275 ppmV (Barnola and others, 1987) to the current level of approx 365 ppmV (Keeling and Whorf, 1998; Keeling, 1994). Carbon dioxide is a significant greenhouse gas as evidenced by infrared absorption bands in light passing through the Earth's atmosphere. Vostok ice-core studies indicate a high correlation between atmospheric pCO_2 levels and ice δD, a proxy for climate, during the glacial (lower pCO_2) and interglacial intervals (higher pCO_2) of the last 160 kyr (Barnola and others, 1987). Knowledge of past carbon dioxide levels and associated paleoenvironmental and paleoecologic changes are useful as a predictive tool for future consequences of the current increases in atmospheric carbon dioxide.

Several techniques have been used to investigate the Earth's history of carbon partitioning and atmospheric CO_2. Tajika and Matsui (1992) estimated atmospheric pCO_2 over Earth's entire history by modeling mantle evolution and the carbon cycle. GEOCARB II and its predecessors are geochemical models that estimate Phanerozoic pCO_2 levels by tracking geological and biological factors such as land area and elevation, plant evolution, and global tectonism (Berner, Lasaga, and Garrels, 1983; Berner, 1991, 1994). Cerling (1991) introduced a CO_2 paleobarometer utilizing $\delta^{13}C$ of pedogenic carbonates. Yapp and Poths (1992, 1996) have estimated paleo-pCO_2 levels by analyzing pedogenic goethites. Differences in $\delta^{13}C$ between associated marine organic matter and carbonates have been related to paleo-pCO_2 levels (Popp and others, 1989; Freeman and Hays, 1992; Pagani, Freeman, and Arthur, 1999; Pagani, Arthur, and Freeman, 1999), and White and others (1994) examined the $\delta^{13}C$ of peat constituents to reconstruct paleo-pCO_2 over the last 14 ky. Worsley and others (1994) have estimated paleo-pCO_2 levels by modeling the latitudinal distributions and areas of land masses over the last 500 my. The relationship between plant morphology (stomatal and cuticular parameters) and pCO_2 has been used to infer paleo-pCO_2 levels from fossil plants (Kürschner and others, 1996; McElwain and Chaloner, 1996). Each of these methods has a different sensitivity

* Department of Geology and Geophysics, University of Utah, Salt Lake City, Utah 84112
** Department of Geology, University of California, Davis, California 95616

range, assumptions, and limitations providing independent means of evaluating paleoatmospheres.

The purpose of this study is to constrain the history of atmospheric pCO_2 over the last 400 my using a paleosol CO_2 paleobarometer (Cerling, 1991). We will first review the theory and assumptions behind the CO_2 paleobarometer and discuss the characteristics of appropriate paleosols. The database of paleosol isotope analyses and calculated pCO_2 results are then presented and compared to the results of other methods with a discussion of geological factors associated with the history of atmospheric CO_2.

TERMINOLOGY AND METHODS

The term pedogenic carbonate is used here to refer to micritic calcite precipitated from solution during active soil formation (in the sense of Jenny, 1941), while the soil is in direct communication with the atmosphere. We have attempted to avoid carbonates precipitated or modified subsequent to soil genesis. Micritic carbonates for analysis were isolated from pedogenic nodules and rhizoliths. The Cerling laboratory results were obtained by homogenizing 3 to 5 mg of pedogenic carbonate and extracting CO_2 by the method of McCrea (1950). Data from the Montañez lab were obtained with 0.2 to 1.0 mg samples using a microdrill and common acid bath at 90°C (method of Bemis and others, 1998). Isotope values are reported in the "δ" notation relative to the Pee Dee Belemnite standard (PDB) with an uncertainty of ±0.1 permil.

Analyses of paleosols presented in other studies are compiled in this report. Only those data that we understand conform to the materials and methods outlined in this study have been included. Data gathered from the literature were treated with the methods and assumptions stated here and do not necessarily yield equivalent pCO_2 results, where applicable, to those of the reporting investigators. Analytical results from 15 modern soils and 758 paleosols are summarized and used in the pCO_2 calculations. The paleosol isotope database presented here represents 365 previously unpublished analyses and 393 analyses gathered from the literature.

PALEOSOLS

Paleosols must meet certain explicit criteria, detailed below, to be of use with the CO_2 paleobarometer. Appropriate paleosols include (nodular) Calcisols, calcic Argillisols, and morphologically similar paleosols of the Mack, James, and Monger (1993) classification system. Analogous modern soils meeting these criteria include the Aridisols (desert/shrub soils), Alfisols (forest soils), and Mollisols (grassland soils) of the United States soil classification system (Soil Survey Staff, 1983).

Recognition of paleosols.–Paleosols discussed in this study are the remains of soils, in the sense of Jenny (1941), formed on land surfaces in ancient times by the subaerial modification of rock or sediment (typically alluvium) through a diverse array of processes (Retallack, 1988, 1990). These processes include plant and animal activities, moisture and temperature fluctuations, leaching, chemical and particle translocations, and mineralogical changes. The operation of these and other processes over hundreds to thousands of years or longer results in the formation of structures and arrangements of materials in a manner unique to soils. The primary features of soils are soil horizons and ped structures, which form at the expense of parent rock or sediment fabrics (Buol, Hole, and McCracken, 1989).

Soils are composed of a vertical succession of horizons, which are a vertical series of morphologically and chemically distinct zones formed by the persistent action of soil processes. Carbonates analyzed for this study formed in calcic horizons at >50 cm depth in the soil. Discussions on the terminology and range of common soil horizons can be found in many soil genesis texts (for example Buol, Hole, and McCracken, 1989). Peds, or soil clods, are units of soil matrix bounded by clay coatings or other segregating

material, with shapes ranging from small sub-millimeter granules to columns extending nearly a meter in depth (Soil Survey Staff, 1983). The types of paleosols used in this study commonly have angular blocky peds ranging from 1 to 5 cm. Eroding paleosols often crumble apart along ped surfaces. Compaction, cementation, and recrystallization can further alter paleosol characteristics from the original soil textures (Retallack, 1990).

The outcrop appearance of a Permian paleosol from the Cedar Mesa formation in southern Utah is illustrated in figure 1. A typical association of alluvial sediments and paleosols is diagrammed in figure 2, depicting stacked paleosols developed on channel and splay sands interbedded with muddy overbank deposits. Soils often develop on floodplain surfaces until erosion by migrating channels or sedimentation halts further soil development.

Pedogenic carbonate.–Calcite accumulations are common in modern soils of equatorial to temperate latitudes with dry climates, where evapo-transpiration exceeds precipitation (Gile, Peterson, and Grossman, 1966). Calcium ions, the weathering product of soil minerals and/or eolian dust, are transported down into the soil profile in solution until precipitated or carried into groundwater. Several factors contribute to the precipita-

Fig. 1. A paleosol from the Permian Cedar Mesa formation in southern Utah. The upper part of the paleosol may have been eroded prior to deposition of the eolian sandstone. Distribution and morphology of the pedogenic carbonate indicate roots are a major control on mineralization. The pick is 65 cm in length.

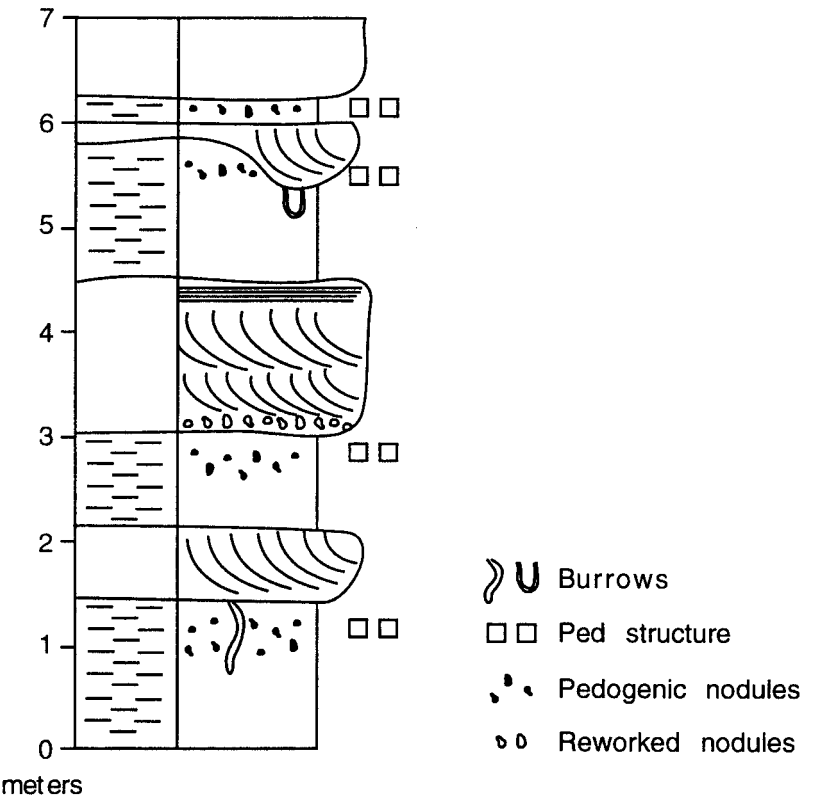

Fig. 2. A stratigraphic representation of paleosols, from the Triassic Dolores formation in Colorado, appropriate for application of the soil carbonate paleobarometer. Paleosols are commonly formed on floodplain surfaces of fluvial basins, forming stacked sequences of paleosols through time.

tion of carbonate at depth in the soil, including water loss, pCO_2 gradients, and temperature changes. The ubiquitous association of pedogenic carbonates with macroscopic and microscopic root structures is an indicator of the importance of biologic factors in its formation, with water loss during evapotranspiration probably being the most important aspect. Many pedogenic carbonate accumulations occur at depths greater than 50 cm in the soil, forming cylindrical to nodular morphologies associated with rooting structures. Internally, pedogenic carbonates are predominantly micritic, with tubular structures, radial veins, and concentric arcs of sparite (fig. 3). These masses often have complex internal structures that apparently represent many generations of carbonate accumulation during the formation of the soil. Prolonged periods of carbonate accumulation can produce thick indurated horizons with brecciation and/or laminated carbonates; such soils may violate assumptions required for the paleobarometer and should be avoided.

Inappropriate paleosols.–Not all pedogenic carbonates are appropriate for use with the CO_2 paleobarometer. Pedogenic carbonates formed under anaerobic or waterlogged conditions are not appropriate. Carbonates precipitated at or near the soil paleo-surface (less than approx 50 cm depth) are not used. Immature paleosols corresponding to Protosols (Mack, James, and Monger, 1993) with intact sedimentary structures or bedding are inappropriate due to insufficient accumulations of carbonates. Paleosols formed on carbonate-rich matrix should be avoided, unless it can be demonstrated that

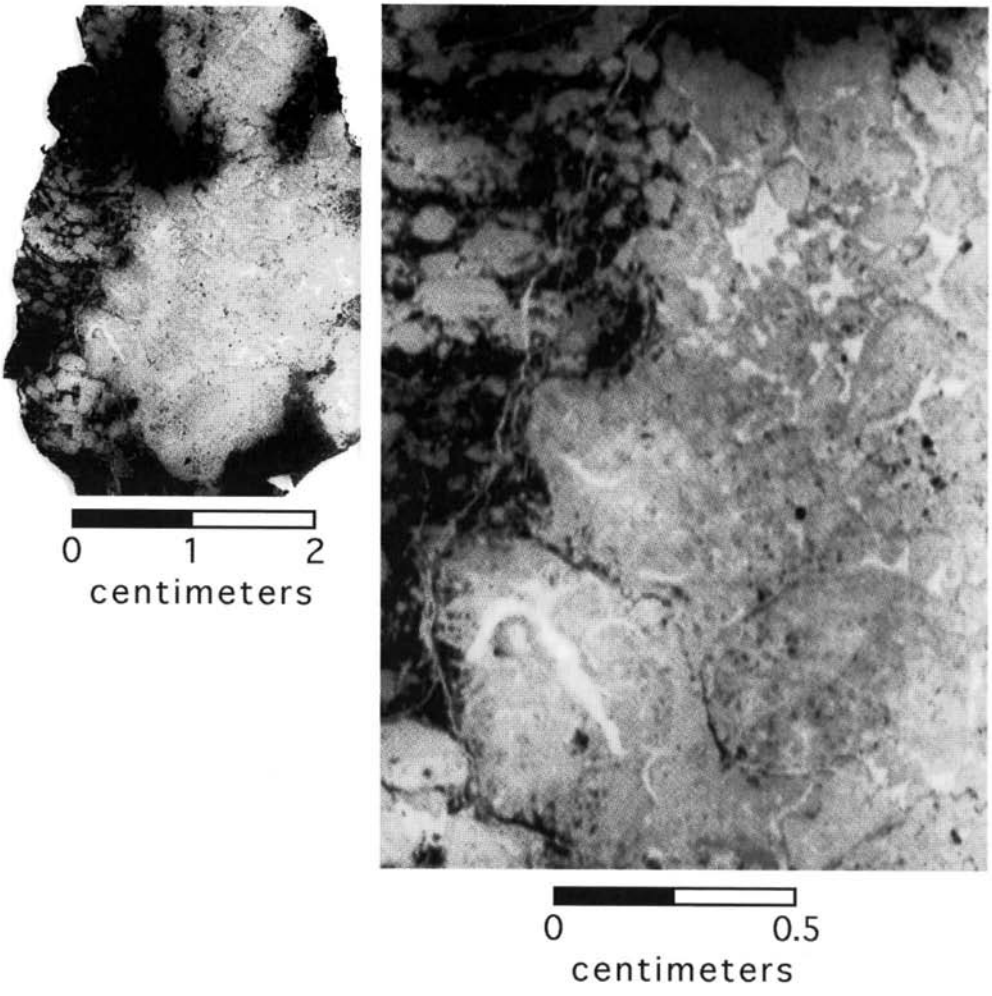

Fig. 3. Two views of a sliced pedogenic carbonate nodule and surrounding matrix from the Glance formation, Arizona, in reflected light. Millimeter to centimeter scale micritic spheroids contain arcuate and radial sparite features.

the pedogenic carbonate is free of inherited carbonate and the local matrix is leached of $CaCO_3$. In our experience, paleosols formed during low stands within marine sequences are particularly susceptible to alteration. Carbonate accumulations must be present in the profile with morphologies that exclude a burial diagenesis or groundwater origin. Examples of inappropriate materials include veins, radiating crystals, septarian nodules, coalballs, and bodies that crosscut lithified soil features.

ATMOSPHERIC CO_2 PALEOBAROMETER

Geochemical modeling and field observations of modern soils indicate that a relationship exists between the $\delta^{13}C$ of pedogenic carbonate and $\delta^{13}C$ and pCO_2 of the atmosphere. The $\delta^{13}C$ of fossil pedogenic carbonates can therefore be used to infer the pCO_2 of paleoatmospheres.

Theory.–Derivation of the CO_2 paleobarometer equation can be broken into several steps. First, a diffusion-production equation is used to model the contributions of atmospheric and soil respired CO_2 in the soil profile. This relationship is then solved with appropriate boundary conditions and modified to reflect the isotopic composition of components. Finally, the terms are rearranged to solve for atmospheric CO_2. The detailed derivation has been published previously (Cerling, 1991; Cerling and Quade, 1993) and will be briefly summarized here.

The diffusion-production equation applied to soil CO_2 is:

$$\frac{\partial C_s}{\partial t} = D_s \frac{\partial^2 C_s}{\partial z^2} + \phi_s(z)$$

where C_s is soil CO_2, t is time, D_s is the diffusion coefficient, and ϕ_s is the production function with respect to depth z (Baver, Gardner, and Gardner, 1972; Kirkham and Powers, 1972; Cerling, 1984). Solving this equation with a no-flux boundary at depth and $C_s(z = 0)$ set equal to atmospheric carbon dioxide yields:

$$C_s(z) = S(z) + C_a$$

where S(z) is CO_2 contributed by soil respiration, and C_a is atmospheric CO_2. Cerling (1984, 1991) solved this equation for ^{12}C and ^{13}C and showed that the isotopic composition of soil CO_2 is controlled by diffusional mass transfer and production. In soils or paleosols with pedogenic $CaCO_3$ precipitated in equilibrium with soil CO_2, the $\delta^{13}C$ value of this $CaCO_3$ can be interpreted as a paleo-ecology indicator or used for pCO_2 barometer calculations. Soil respired CO_2 in C_3 plants is depleted approx 18 permil relative to atmospheric CO_2 because of diffusional processes and isotope fractionations during photosynthesis (Farquhar, Ehleringer, and Hubic, 1989). The solution to the soil CO_2 equation of Cerling (1984, 1991, 1999) can be recast in terms of the isotopic composition of atmospheric CO_2:

$$C_a = S(z)\frac{\delta^{13}C_s - 1.0044\delta^{13}C_\phi - 4.4}{\delta^{13}C_a - \delta^{13}C_s} \quad (1)$$

by using the assumption that $^{12}C_s/^{12}C_a \approx C_s/C_a$ (Davidson, 1995) where $\delta^{13}C_s$, $\delta^{13}C_\phi$, and $\delta^{13}C_a$ are the isotopic composition of soil CO_2, soil respired CO_2, and the atmosphere respectively. The term S(z) is a function of depth but approaches a constant value below about 20 to 30 cm depth (Cerling, 1984; Cerling and Quade, 1993). Soil CO_2 is enriched in ^{13}C relative to respired CO_2 by 4.4 permil due to mass dependent rates of diffusion (Cerling and others, 1991), independent of CO_2 concentration.

We assume that pedogenic carbonate forms in isotopic equilibrium with soil gas throughout the soil profile (Cerling, 1992; Cerling and Quade, 1993). The isotopic composition of soil CO_2 is calculated from the isotopic composition of pedogenic carbonate using the temperature dependent fractionation factor of Romanek, Grossman, and Morse (1992). We assume the respiration rate of the soil as well as the isotopic compositions for the atmosphere and soil respired CO_2. These three assumptions produce significant uncertainty in the calculated pCO_2 and are discussed below.

Requirements of the model.–Paleosols used for the CO_2 paleobarometer must meet specific criteria relating to their soil genesis and subsequent diagenetic history. During formation, appropriate soils must be under aerobic, subaerial conditions such that all oxidized carbon species are in isotopic equilibrium and mass transport is diffusion controlled. Samples of pedogenic carbonate need to be collected from greater than approx 50 cm depth in the soil profile to avoid the steep concentration and isotope gradients predicted and observed near soil surfaces (Cerling and Quade, 1993). Samples

for isotopic analysis must be free of non-pedogenic carbonate; sampling is therefore limited to horizons where the matrix is noncalcareous (including matrix-leached zones).

Diagenetic alteration of the original isotopic composition of pedogenic carbonate must be avoided. Evidence of significant recrystallization or metamorphism (such as phyllitic textures and sparry calcite nodules) preclude a simple application of the paleobarometer, though an analysis of alteration may be possible.

Verification of the model.–Application of the CO_2 paleobarometer to modern soils is a general test of the usefulness and response characteristics of the method. Due to the expansion of C_4 plants in the Late Miocene (Quade and Cerling, 1995; Cerling and others, 1997) there are few examples of modern soils with pedogenic carbonate forming under C_3 ecosystems that serve as modern analogs to the paleosols in this study. C_4 plants outcompete C_3 plants at high temperatures and low pCO_2 concentrations (Cerling, Ehleringer, and Harris, 1998). We therefore lack ideal modern analogs for warm climate soils accumulating calcium carbonate under pure C_3 vegetation. However modern soils with pedogenic carbonate and C_3 vegetation do form in restricted areas with cool growing seasons.

The CO_2 paleobarometer is applied to those modern soils reported in Cerling and Quade (1993) that developed on post-glacial sediments and have $\delta^{13}C_{om}$ values of −23 permil or less representing C_3 vegetation. Mean growing season temperatures for these soils are estimated from local weatherstations or the global temperature dataset of Pearce and Smith (1984). Calculated pCO_2 values (table 1) range from −30 to 1000 ppmV. Negative numbers result from the mathematics and probably represent pCO_2 levels less than 500 ppmV. An atmospheric pCO_2 level of approx 280 ppmV for modern soils is expected, based on ice core studies (Wahlen and others, 1993; Barnola and others, 1987). When treated statistically, the average (433 ppmV ± 385 1σ) is higher than the expected result; however, it is within a standard deviation of the modern atmospheric condition. The results for calculations on analyses from paleosols are treated similarly, with the average value from each formation being presented as the corresponding atmospheric

TABLE 1

Isotope data from modern pedogenic carbonates and soil organic matter, the difference between $\delta^{13}C$ carbonate and $\delta^{13}C$ organic matter, the mean growing season temperature, isotopic composition of CO_2 contributed by soil respiration, isotopic composition of atmospheric CO_2, estimated contribution of respired CO_2 and calculated atmospheric pCO_2. Isotope data from Cerling and Quade (1993) and unpublished

Soil	Region	$\delta^{13}C_{cc}$ (permil)	$\delta^{13}C_{om}$ (permil)	$\Delta_{cc\text{-}om}$ (permil)	T_{mgs} (°C)	$\delta^{13}C_s$ (permil)	$\delta^{13}C_a$ (permil)	S(z) (ppmV)	pCO_2 (ppmV)
Salla	Bolivia	−8.5	−23.3	14.8	11	−19.0	−6.5	5000	0
Provence	France	−10.0	−25.0	15.0	12	−20.1	−6.5	5000	120
Samos	Greece	−9.3	−25.7	16.4	14	−19.3	−6.5	5000	760
Axios	Greece	−7.5	−23.7	16.2	14	−17.5	−6.5	5000	780
SM-5	Nevada	−8.5	−23.7	15.2	7	−18.7	−6.5	5000	−30
SM-6	Nevada	−8.5	−23.9	15.4	6	−18.7	−6.5	5000	0
SM-4	Nevada	−6.8	−23.4	16.6	8	−17.0	−6.5	5000	380
Howard	New York	−9.4	−25.6	16.2	16	−18.8	−6.5	5000	780
Elstow	Saskatchewan	−7.9	−24.2	16.3	15	−18.0	−6.5	5000	860
Sask-1	Saskatchewan	−8.4	−24.1	15.7	15	−18.5	−6.5	5000	570
Pasalar-1	Turkey	−10.0	−24.5	14.5	18	−19.9	−6.5	5000	200
Pasalar-2	Turkey	−10.3	−24.5	14.2	18	−20.2	−6.5	5000	90
Dimple Dell	Utah	−7.4	−24.5	17.1	11	−17.6	−6.5	5000	1000
Big Cottonwood	Utah	−7.5	−24.4	16.9	11	−17.7	−6.5	5000	900
Parley Canyon	Utah	−8.8	−23.8	15.0	11	−19.0	−6.5	5000	80
								Average	433
								1σ	385

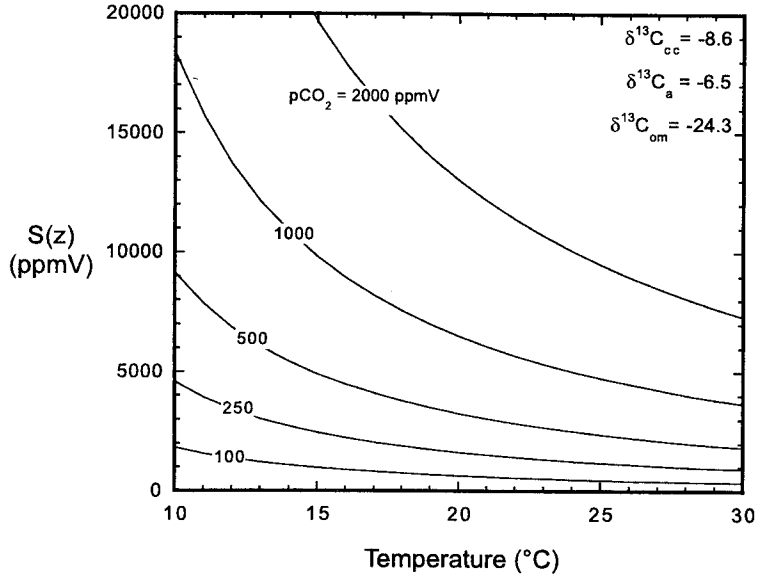

Fig. 4. Effects of varying temperature and S(z) on calculated carbon dioxide concentrations from 0 to 2000 ppmV. The isotopic compositions of the atmosphere, organic matter, and soil carbonate (based on averages of available modern soil data) are held constant.

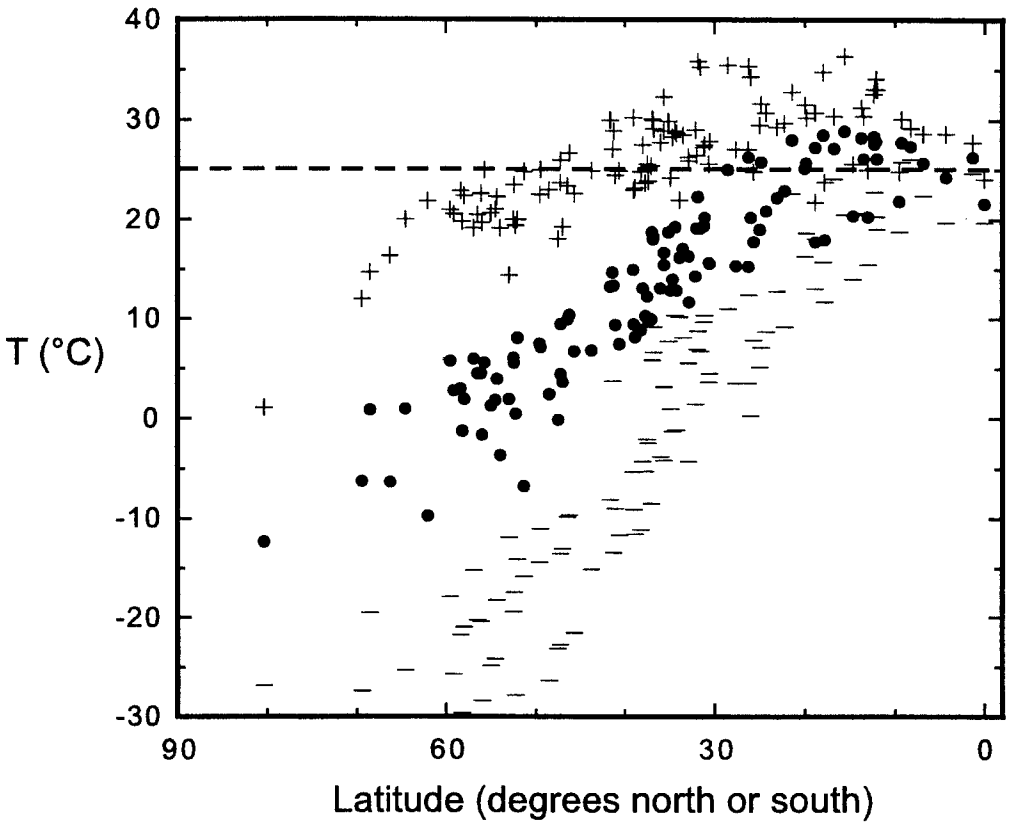

Fig. 5. The average monthly temperatures of Europe, Asia, and Africa (IAEA/WMO, 1998) plotted by latitude. The mean average monthly temperature (solid circle), highest average monthly temperature (+), and lowest average monthly temperature (−) are plotted for each station. A temperature of 25°C was used for pCO_2 calculations.

pCO_2. The sensitivity of the model changes with atmospheric pCO_2, due to differing contributions of atmospheric CO_2 to soil CO_2.

EVALUATION OF PARAMETERS

Physical conditions in soils fluctuate due to diurnal and seasonal cycles and associated changes in temperature and moisture. It is probable that ancient paleoenvironments ranged beyond the conditions represented by soils on the modern landscape. Since we are unable to measure directly the variables required for each pCO_2 calculation, we use assumptions where necessary.

Soil respired CO_2.–The concentration of soil respired CO_2, S(z), is a function of depth, though it reaches a nearly constant value below 50 cm depth, where carbonates are commonly precipitated (Cerling and Quade, 1993). The S(z) of fossil soils at carbonate forming depths is an important, yet unknown quantity for calculating paleo-pCO_2. S(z) is a function of the respiration rate, porosity, tortuosity, and the characteristic depth of production (Kirkham and Powers, 1972). Note in eq (1) that, leaving other variables constant, the calculated pCO_2 is directly proportional to S(z). Our lack of knowledge of the respired CO_2 concentration for these fossil soils is one of the major sources of uncertainty with this method.

Modern soils show a large range of respiration rates from none in sterile soils up to more than 8 mmoles/m^2/hr in highly productive soils (Singh and Gupta, 1977). These rates vary through space and time with changes in the conditions that control productivity such as temperature and precipitation. A constant respiration rate is assumed for the paleosols utilized in this study, justified by the restricted range of soil types represented. Studies of modern soils (Solomon and Cerling, 1987; Brook, Folkoff, and Box, 1983; Quade, Cerling, and Bowman, 1989; and Cerling, unpublished data) suggest that S(z) ranges between about 4000 and 7000 ppmV at and below 50 cm depth for soils meeting our criteria of being well drained and having mean annual precipitation below 100 cm. We have therefore chosen a S(z) of 5000 ppmV for all our calculations. The effect of S(z) and temperature on pCO_2 calculations is illustrated in figure 4.

Temperature.–Isotopic fractionation factors for reactions in the CO_2–H_2O–$CaCO_3$ system vary with temperature, such that uncertainties of paleotemperature lessen the precision of pCO_2 calculations. Though we cannot directly measure the paleotemperatures of the fossil soils during carbonate formation, we infer them by analysis of temperatures in modern soils with similar morphologies.

The paleosols presented in this study formed in paleolatitudes corresponding to modern temperate and subtropical zones. Modern growing season temperatures at elevations below 1500 m in these low to mid-latitudes typically range from 10° to 30°C (Pearce and Smith, 1984). The temperature range at 50 cm depth in a soil is less than the surface extremes due to the heat capacity of soil materials and attenuation of temperature extremes from the surface by heat diffusion. A plot of mean monthly temperatures by latitude (fig. 5, data from IAEA/WMO, 1998) demonstrates that, for the modern condition, 25°C is a typical average monthly temperature for subtropical regions as well as a typical maximum monthly temperature for the temperate latitudes. Global temperature changes in the past are thought to be most extreme at high latitudes with diminishing changes at lower latitudes, where the paleosols presented in this study formed. We have therefore chosen 25°C as a constant temperature of formation for all the pedogenic carbonates. The carbon dioxide to calcite carbon isotope enrichment factor is approx 9 permil at 25°C (Romanek, Grossman, and Morse, 1992).

Organic matter.–We assume that the carbon isotope composition of bulk organic matter (OM) in soils and paleosols is equivalent to the isotopic composition of soil respired CO_2, ϕ, a variable required for this method of calculating pCO_2. The mass fraction of OM in modern soils is much higher than that of most analogous fossil soils, especially for the well aerated types of soils and paleosols we discuss here. The mass of OM of an active soil rapidly decreases once a soil becomes buried or sterile (Balesdent and Mariotti, 1996). After the oxidation and metabolism of most of the soil OM, it is likely that

the remaining organic matter is no longer representative of the original material, due to differential rates of oxidation and metabolism for different species (Nadelhofer and Fry, 1988). Possible contamination of fossil OM with modern OM during erosion of overlying sediments and exposure of the paleosols is an additional complication. Compound specific analyses may help eliminate these difficulties in future studies.

Rather than measure the remains of fossil organic matter from the paleosols, we calculated a proxy record, derived from the fossil record of marine carbonates (Veizer and others, 1999), for the isotopic compositions of the atmosphere and soil organic matter. The uppermost ocean and atmosphere mix vigorously over much of the Earth's surface, maintaining near equilibrium conditions between carbon species in these reservoirs (Lynch-Stieglitz and others, 1995). Evidence for the maintenance of this relationship is provided by a nearly constant isotope gradient between contemporaneous marine and terrestrial fossils over geologic time as well as carbon isotope excursions in equivalent marine and terrestrial sequences (Koch, Zachos, and Dettman, 1995; Sinha and Stott, 1994). We assume that the difference in isotopic composition between surface ocean carbonates and the atmospheric carbon dioxide ($\delta^{13}C_{occ}$-$\delta^{13}C_{atm}$) is 8 permil based on the isotopic composition of pre-industrial carbon dioxide trapped in glacial ice (Friedli and others, 1986) and contemporaneous surface ocean carbonates (Veizer and others, 1999; Shackleton and others, 1983). Due to difficulties in dating terrestrial sequences, the geologic record of surface ocean carbonates of Veizer and others (1999) was smoothed prior to being used for calculation of proxy records for the isotopic composition of the atmosphere and OM (fig. 6).

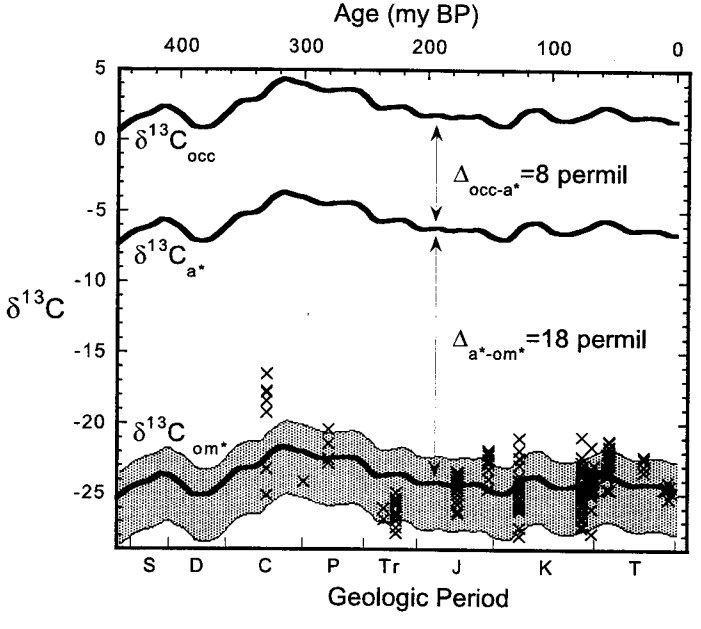

Fig. 6. The isotopic compositions of surface ocean carbonates and derived proxy records utilized in our pCO_2 calculations, assuming constant differences between the carbon isotope compositions of surface ocean carbonates, atmospheric carbon dioxide, and soil organic matter. The top curve illustrates surface ocean carbonates (modified by smoothing the results of Veizer and others, 1999). The middle curve is the proxy record used for the isotopic composition of atmospheric CO_2. The stippled area represents the expected range, due to environmental variables such as water stress and canopy recycling, of soil organic matter. The line within the stippled zone is our proxy record for soil organic matter for soils accumulating pedogenic carbonate. Measured terrestrial organic matter values from Bocherens and others (1993), Jones (1994), and Ekart and Cerling (unpublished) are plotted (x) for comparison to the calculated values.

Usefulness of the CO_2 paleobarometer is reduced with ecosystems containing C_4 organic matter (fig. 7), due to the diminished difference in isotopic composition between atmospheric carbon dioxide and OM. We assume that all the paleosols developed under pure C_3 ecosystems, lacking evidence for significant C_4 or CAM biomass prior to about 8 my (Quade and Cerling, 1995). For paleosols younger than 8 my, isotopic analyses of organic matter and fossil bioapatite were used to restrict our study to paleosols that formed under C_3 ecosystems, though proxy values were used for pCO_2 calculations. The difference in carbon isotope composition between tropospheric carbon dioxide and OM is produced by discrimination against ^{13}C during photosynthesis. The magnitude of this isotopic gradient varies significantly with ecologic conditions. We assume that the fractionation between atmospheric carbon dioxide and soil OM ($\delta^{13}C_a$-$\delta^{13}C_{om}$) for the paleosols presented here is 18 permil based on the range of modern C_3 ecosystem fractionations (Buchmann and others, 1998). The isotopic compositions of fossil land plants (Degens, 1969; Bocherens and others, 1993; Jones, 1994; Ekart and Cerling unpublished data) are plotted in figure 6 for comparison to the calculated proxy record.

Uncertainties.–The nature of the data set makes it difficult to place quantitative error margins on the pCO_2 estimates, and Cerling (1992) has discussed the problems of this method. Sensitivity of the model decreases at lower pCO_2 concentrations such that the structure of the data below 1000 ppmV is possibly noise. Improvements in any or all of the assumed variables would aid in better estimates of pCO_2. We have presented an upper and lower uncertainty estimate based on calculating a pCO_2 value one standard deviation above and below the average $\delta^{13}C_{cc}$ for each formation.

RESULTS AND DISCUSSION

Analytical data from the paleosol carbonates, $\delta^{13}C$ proxy values, and results of calculations are summarized in tables 2, 3 and 4. Data are grouped by formation, with further division for multiple data sources or deposition across an epoch or period

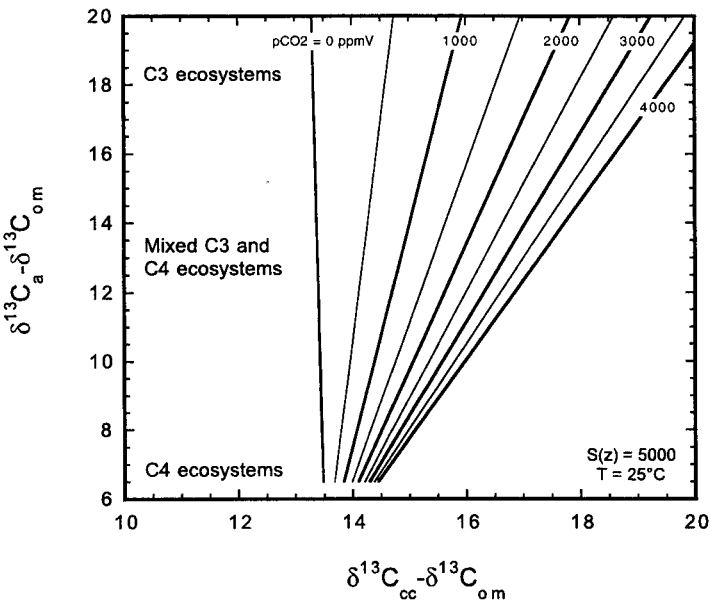

Fig. 7. Effectiveness of the CO_2 paleobarometer with varying contributions of biomass from C_4 photosynthesis. Sensitivity to atmospheric carbon dioxide decreases with increasing C_4 biomass due to a smaller carbon isotope difference between atmospheric carbon dioxide and organic matter.

TABLE 2

Sample data from Cenozoic paleosol bearing formations, sample age, $\delta^{13}C$ of pedogenic carbonates, standard deviation, number, $\delta^{13}C$ of contemporary surface ocean carbonates (estimated from Veizer and others, 1999), calculated $\delta^{13}C$ of the atmosphere and organic matter, the quantity $\delta^{13}C_{cc}-\delta^{13}C_{om^*}$, and calculated paleoatmospheric pCO_2

Formation or Identifier	Age (my)	$\delta^{13}C$ (permil)	1σ (permil)	n	$\delta^{13}C_{occ}$ (permil)	$\delta^{13}C_{a^*}$ (permil)	$\delta^{13}C_{om^*}$ (permil)	$\Delta_{cc\text{-}om^*}$ (permil)	pCO_2 (ppmV)	Source of Isotope Data
Rhodes	3	−8.8	1.3	6	1.4	−6.6	−24.6	15.8	1170	Quade, Solounias, and Cerling, 1994
Messinian	5	−9.5	0.7	3	1.5	−6.5	−24.5	15.0	810	this study**
Mytilini	6	−9.6	0.8	7	1.5	−6.5	−24.5	14.9	730	Quade, Solounias, and Cerling, 1994
Dhok Pathan	7	−10.4	1.5	13	1.5	−6.5	−24.5	14.1	370	Quade and Cerling, 1995
Nagri	9	−10.0	0.7	13	1.6	−6.4	−24.4	14.4	510	Quade and Cerling, 1995
Nea Messimbria	10	−8.7	0.9	8	1.6	−6.4	−24.4	15.7	1120	Quade, Solounias, and Cerling, 1994
Pikermi	10	−8.6	0.3	2	1.6	−6.4	−24.4	15.8	1170	Quade, Solounias, and Cerling, 1994
Chinji	13	−9.4	0.3	11	1.7	−6.3	−24.3	14.9	740	Quade and Cerling, 1995
Kamlia	13	−10.1	0.9	6	1.7	−6.3	−24.3	14.3	440	Quade and Cerling, 1995
Fort Ternan	14	−11.8	1.3	10	1.7	−6.3	−24.3	12.5	−220	Cerling and others, 1991
Huete	21	−9.3	0.5	2	1.7	−6.3	−24.3	15.0	780	this study**
Salla	25	−8.0	1.0	5	1.8	−6.3	−24.3	16.3	1470	T. E. Cerling and B. J. MacFadden***
Claron	45	−6.9	0.5	4	2.1	−5.9	−23.9	17.0	1950	this study**
Willwood	55	−8.5	0.6	33	2.4	−5.6	−23.6	15.1	820	Koch, Zachos, and Dettman, 1995
Willwood	55	−10.6	1.0	49	2.4	−5.6	−23.6	13.0	−60	Cerling, 1992
Argiles Plastiques Bariolées	55	−10.5	1.5	6	2.4	−5.6	−23.6	13.1	−20	Sinha and Stott, 1994
Fort Union/Willwood	57	−8.0	1.1	56	2.4	−5.6	−23.6	15.6	1070	Koch, Zachos, and Dettman, 1995
Argiles Plastiques Bariolées	57	−9.3	1.1	18	2.4	−5.6	−23.6	14.3	460	Sinha and Stott, 1994
Javelina/Black Peaks	65	−10.9	0.6	31	2.2	−5.8	−23.8	12.9	−90	this study**

* Inferred value, ** Cerling laboratory, *** unpublished data.

TABLE 3

Sample data from Mesozoic paleosol bearing formations and associated data as in Table 2

Formation or Identifier	Age (my)	$\delta^{13}C$ (permil)	1σ (permil)	n	$\delta^{13}C_{occ}$ (permil)	$\delta^{13}C_{a^*}$ (permil)	$\delta^{13}C_{om^*}$ (permil)	$\Delta_{cc\text{-}om^*}$ (permil)	pCO_2 (ppmV)	Source of Isotope Data
North Horn	66	−8.8	0.4	6	2.2	−5.8	−23.8	15.1	820	this study**
Javelina	67	−9.7	0.5	36	2.1	−5.9	−23.9	14.2	430	this study**
Provence	67	−9.2	0.3	8	2.1	−5.9	−23.9	14.7	630	this study**
Lameta Beds	68	−10.7	0.8	11	2.1	−5.9	−23.9	13.3	60	Andrews, Tandon, and Dennis, 1995
Lameta Beds	68	−9.1	1.0	19	2.1	−5.9	−23.9	14.9	720	Ghosh, Bhattacharya, and Jani, 1995
Two Medicine	75	−6.0	0.8	10	1.8	−6.2	−24.2	18.3	2950	this study**
Kaiparowitz	80	−8.4	0.7	3	1.7	−6.4	−24.4	15.9	1260	this study**
Proctor Lake	108	−7.1	1.5	5	2.2	−5.8	−23.8	16.7	1750	Cerling, 1991
Cloverly	115	−6.3	0.3	7	2.3	−5.7	−23.7	17.5	2260	this study**
Cedar Mountain	115	−5.7	0.9	9	2.3	−5.7	−23.7	18.0	2710	this study**
Kootenai	115	−5.8	1.3	9	2.3	−5.7	−23.7	18.0	2690	this study**
Glance	120	−7.5	0.6	5	2.2	−5.8	−23.8	16.3	1480	this study**
Morrison	150	−6.2	1.0	63	1.4	−6.7	−24.7	18.5	3180	this study**
Kayenta	175	−4.5	0.5	3	1.8	−6.2	−24.2	19.7	4560	this study**
Aztec	177	−7.3	0.1	2	1.7	−6.3	−24.3	17.0	1920	this study**
McCoy Brook	205	−5.9	0.5	4	1.8	−6.2	−24.2	18.3	3010	Suchecki, Hubert, and Birney de Wit, 1988
New Haven Arkose	210	−5.6	1.7	5	1.9	−6.1	−24.1	18.5	3160	Suchecki, Hubert, and Birney de Wit, 1988
Chinle	220	−7.0	1.5	12	2.4	−5.6	−23.6	16.6	1650	this study**
Dolores	220	−6.7	0.2	6	2.4	−5.6	−23.6	16.9	1830	this study**
Ischigualasto	220	−5.4	1.1	6	2.4	−5.6	−23.6	18.2	2850	I. P. Montañez and J. T. Parrish***
Wolfville	225	−6.4	0.4	3	2.4	−5.6	−23.6	17.2	2060	Suchecki, Hubert, and Birney de Wit, 1988
Otter Sandstone	234	−8.8	0.8	6	2.3	−5.7	−23.7	14.9	710	Purvis and Wright, 1991
Otter Sandstone	234	−9.0	0.5	6	2.3	−5.7	−23.7	14.6	610	this study**

* Inferred value, ** Cerling laboratory, *** unpublished data.

TABLE 4

Sample data from Paleozoic paleosol bearing formations and associated data as in table 2

Formation or Identifier	Age (my)	$\delta^{13}C$ (permil)	1σ (permil)	n	$\delta^{13}C_{occ}$ (permil)	$\delta^{13}C_{a^*}$ (permil)	$\delta^{13}C_{om^*}$ (permil)	$\Delta_{cc\text{-}om^*}$ (permil)	pCO_2 (ppmV)	Source of Isotope Data
Quartermaster	251	−7.4	0.2	6	3.1	−4.9	−22.9	15.5	1000	this study†
Clear Fork Group	273	−4.8	0.7	15	3.6	−4.4	−22.4	17.6	2380	this study†
Organ Rock	275	−3.9	0.9	9	3.6	−4.4	−22.4	18.5	3160	this study**
Waggonner Ranch	276	−5.2	0.9	22	3.6	−4.4	−22.4	17.2	2080	this study†
Petrolia, upper	279	−4.3	0.6	6	3.5	−4.5	−22.5	18.2	2840	this study†
Petrolia, lower	284	−8.2	1.4	13	3.5	−4.5	−22.5	14.3	440	this study†
Cedar Mesa	285	−2.6	0.9	4	3.5	−4.5	−22.5	19.9	4690	this study**
Abo	290	−5.3	1.6	8	3.6	−4.4	−22.4	17.1	1980	Mack and others, 1991
Abo	290	−5.7	1.0	5	3.6	−4.4	−22.4	16.7	1730	this study**
Halgaito	292	−4.0	1.1	12	3.7	−4.3	−22.3	18.3	2960	this study**
Dunkard	293	−8.7	0.4	5	3.7	−4.3	−22.3	13.6	150	Mora, Driese, and Colarusso, 1996
Nocona	294	−8.9	3.0	3	3.8	−4.2	−22.2	13.3	60	this study†
Archer City	296	−10.1	0.7	16	3.8	−4.2	−22.2	12.1	−370	this study†
Naco Group	302	−5.7	0.8	11	4.0	−4.0	−22.0	16.3	1470	Kenny and Neet, 1993
Fountain	303	−5.6	0.4	11	4.0	−4.0	−22.0	16.4	1520	this study**
Conemaugh	305	−7.2	0.6	8	4.0	−4.0	−22.0	14.8	650	Mora, Driese, and Colarusso, 1996
Pennington	325	−7.0	0.5	3	3.9	−4.0	−22.0	15.0	790	Mora, Driese, and Colarusso, 1996
Hinton	326	−7.6	0.8	5	3.9	−4.1	−22.1	14.5	540	Mora, Driese, and Colarusso, 1996
Mauch Chunk	327	−7.0	0.5	5	3.8	−4.2	−22.2	15.2	860	Mora, Driese, and Colarusso, 1996
Terwagne	343	−7.1	0.5	22	2.9	−5.2	−23.2	16.0	1310	Muchez and others, 1993
Clifton Down Mudstone	345	−6.0	0.9	4	2.8	−5.2	−23.2	17.2	2060	this study**
Maccrady	352	−7.6	1.2	9	2.7	−5.3	−23.3	15.7	1110	Mora, Driese, and Colarusso, 1996
Catskill, Duncannon	363	−9.8	0.3	12	1.9	−6.1	−24.1	14.3	470	Mora, Driese, and Colarusso, 1996
Catskill, Sherman Creek	365	−9.0	0.1	5	1.7	−6.3	−24.3	15.3	920	Mora, Driese, and Colarusso, 1996
Old Red Sandstone	380	−8.7	0.2	3	0.9	−7.1	−25.1	16.4	1560	this study**
Bloomsburg	415	−5.3	1.2	9	2.4	−5.6	−23.6	18.3	2980	Mora, Driese, and Colarusso, 1996

* Inferred value, ** Cerling laboratory, † Montañez laboratory.

boundary. Geologic ages were assigned to each formation based on literature searches, stratigraphic relationships, and personal communications with individuals listed in the acknowledgements. Numerical age estimates (table 5) were based on the geologic time scale of Harland and others (1990), modified by the results of Bowring and others (1998) and Rasbury and others (1998). Field locations of the paleosols are given in table 5.

The average $\delta^{13}C_{cc}$ for the formations listed in tables 2, 3, and 4 range from −11.8 to −2.6 permil (illustrated in fig. 8). The isotopic compositions of contemporaneous pedogenic carbonates appear to be similar. For example, the Maastrichtian paleosols of India, France, and the United States (Texas and Utah) all have similar carbon isotopic compositions. Furthermore, the 5 point weighted average of $\delta^{13}C_{cc}$ through time produces a reasonable fit to almost all the data. A good fit to the trend supports the hypothesis that global factors (the isotopic composition and partial pressure of carbon dioxide in the atmosphere) control the isotopic composition of pedogenic carbonates in the types of paleosols studied. The average difference between the isotopic composition of pedogenic carbonate and our proxy organic matter record ($\Delta_{cc\text{-}om^*}$) ranges from 12.1 to 19.9 permil, illustrated in figure 9. This value is proportional to the pCO_2 of the atmosphere.

Geologically short term negative carbon isotope excursions have been observed in both marine and terrestrial components at certain time intervals in the rock record (Margaritz, 1989). It is possible that non-equilibrium conditions exist between labile carbon reservoirs (atmosphere, ocean, and biosphere) during these relatively brief events. Paleosols thought to have formed during the Paleocene/Eocene excursion (Koch, Zachos, and Dettman, 1995; Sinha and Stott, 1994) and the Cretaceous/Tertiary excursion (Ekart and Cerling, unpublished data) were therefore withheld from the database.

Results of the pCO_2 calculations are given in tables 2, 3 and 4 and illustrated in figure 10. A 5 point weighted average for concentrations of CO_2 from individual formations is plotted as a function of time. Results indicate pCO_2 levels ranging from less than 500 ppmV ($RCO_2 \approx 1$, the modern condition) to over 4500 ppmV ($RCO_2 \approx 15$) over the last 415 my. Several oscillations between states of high and low pCO_2 occur over the study interval. The coarse temporal sampling precludes detection of higher frequency oscillations at this time. Calculated pCO_2 for three different assumed temperatures are illustrated in figure 11 to show the effect of temperature on calculations.

Paleozoic.–The oldest paleosols reported in this study are from the Late Silurian Bloomsburg formation (Driese and others, 1992; Mora, Driese, and Colarusso, 1996). These soils were presumably developed under very primitive vascular plants (Stewart, 1983), which may have been incapable of producing soil conditions meeting our assumptions, especially regarding respiration rate. Overestimation of soil respiration rates, for these possibly low productivity soils, would lead to overestimation of pCO_2. The high pCO_2 levels calculated for these soils should therefore be considered tentative. A decline in pCO_2 levels interpreted for the Paleozoic (Mora, Driese, and Colarusso, 1996; Mora and Driese, 1993; Mora, Driese, and Seager, 1991) are largely based on analyses of these Late Silurian paleosols. A downward trend is apparent in the results presented here, and higher pCO_2 levels in the Early Paleozoic have been indicated by independent methods (Yapp and Poths, 1996; Berner, 1994; Worsley and others, 1994). Evolution and expanded distribution of vascular plants has been hypothesized to be a factor in the Paleozoic decrease in pCO_2 (Berner, 1997, 1992).

Devonian, Carboniferous, and Earliest Permian indicate relatively low pCO_2 (at approx 1000 ppmV). This suggests that the vast quantities of carbon stored in carbonates, marine shales, and coals were offset by other processes releasing carbon to the atmosphere. Calculated pCO_2 levels from Permian paleosols show a large range of values. The abrupt increase in pCO_2 in the Early Permian corresponds to changes in

TABLE 5

Formation or Identifier	Stratigraphic Age	Age (my)	Location
A. *Cenozoic paleosol bearing sediments, their ages, and locations.*			
Rhodes	Pliocene	3	Greece
Messinian	Miocene	5	Provence, France
Mytilini	Miocene	6	Samos, Greece
Dhok Pathan	Miocene	7	Kaulial Kas, Pakistan
Nagri	Miocene	9	Pakistan
Nea Messimbria	Miocene	10	Chios, Greece
Pikermi	Miocene	10	Greece
Chinji	Miocene	13	Pakistan
Kamlial	Miocene	13	Gabhir Kas, Pakistan
Fort Ternan	Miocene	14	Rift Valley, Kenya
Huete	Miocene	21	Spain
Salla	Oligocene	25	Bolivia
Claron	Eocene	45	Utah
Willwood	Eocene	55	Wyoming
Fort Union	Paleocene	57	Wyoming
Argiles Plastiques Bariolées	Paleocene	57	Paris Basin, France
Black Peaks	Paleocene	65	Big Bend, Texas
B. *Mesozoic paleosol bearing sediments, their ages, and locations.*			
North Horn	Maastrichtian	66	Utah
Javelina	Maastrichtian	67	Big Bend, Texas
Provence	Maastrichtian	67	France
Lameta Beds	Maastrichtian	68	India
Two Medicine	Campanian	75	Choteau, Montana
Kaiparowits	Campanian	80	Utah
Proctor Lake	Albian	108	Texas
Cloverly	Aptian	115	Wyoming
Cedar Mountain	Aptian	115	San Rafael Swell, Utah
Kootenai	Aptian	115	Montana
Glance	Aptian	120	Arizona
Morrison	Kimmeridgian	150	Western United States
Kayenta	Early Jurassic	175	Utah
Aztec	Aalenian	177	Nevada
McCoy Brook	Hettangian	205	Connecticut
New Haven Arkose	Norian	210	Connecticut
Chinle	Carnian/Norian	220	Western United States
Dolores	Carnian/Norian	220	Colorado
Ischigualasto	Carnian/Norian	220	Argentina
Wolfville	Carnian/Norian	225	Connecticut
Otter Sandstone	Anisian/Ladinian	234	United Kingdom
C. *Paleozoic paleosol bearing sediments, their ages, and locations.*			
Quartermaster	Ochoan	251	Texas
Clear Fork Group	Late Leonardian	273	Texas
Organ Rock	Leonardian	275	Utah
Waggonner Ranch	Middle Leonardian	276	Texas
Petrolia, upper	Early Leonardian	279	Texas
Petrolia, lower	Wolfcampian	284	Texas
Cedar Mesa	Late Wolfcampian	285	Utah
Abo	Wolfcampian	290	New Mexico
Halgaito	Wolfcampian	292	Utah
Dunkard	Early Permian	293	Eastern United States
Nocona	Wolfcampian	294	Texas
Archer City	Wolfcampian	296	Texas
Naco Group	Late Pennsylvanian	302	Arizona
Fountain	Pennsylvanian	303	Colorado
Conemaugh	Pennsylvanian	305	Eastern United States
Pennington	Late Mississippian	325	Eastern United States
Hinton	Late Mississippian	326	Eastern United States
Mauch Chunk	Visean/Namurian	327	Eastern United States
Terwagne	Early Visean	343	Belgium
Clifton Down Mudstone	Chadian/Arundian	345	United Kingdom
Maccrady	Mississippian	352	Eastern United States
Catskill, Duncannon	Famennian	363	Pennsylvania
Catskill, Sherman Creek	Late Devonian	365	Eastern United States
Old Red Sandstone	Middle Devonian	380	United Kingdom
Bloomsburg	Ludlovian/Pridolian	415	Pennsylvania

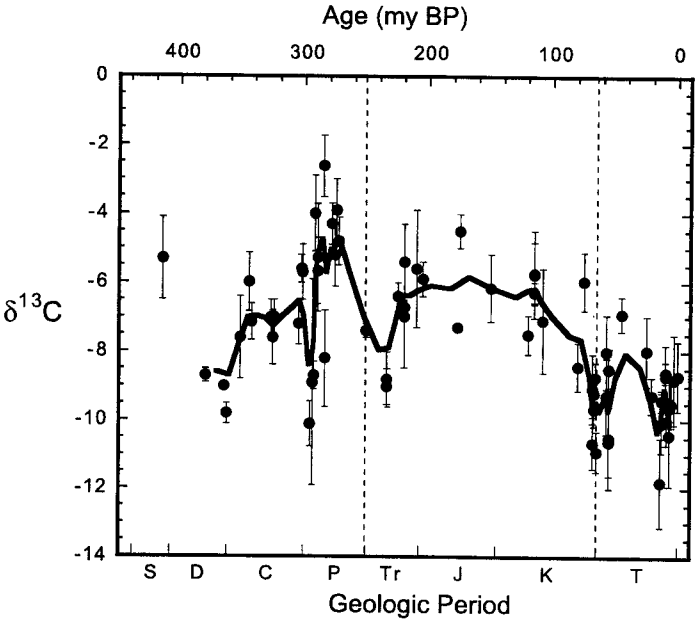

Fig. 8. Isotopic composition of pedogenic carbonates. Averages for each formation are plotted with standard deviation (1σ) bars. The curve represents a 5 point weighted running average for the data points.

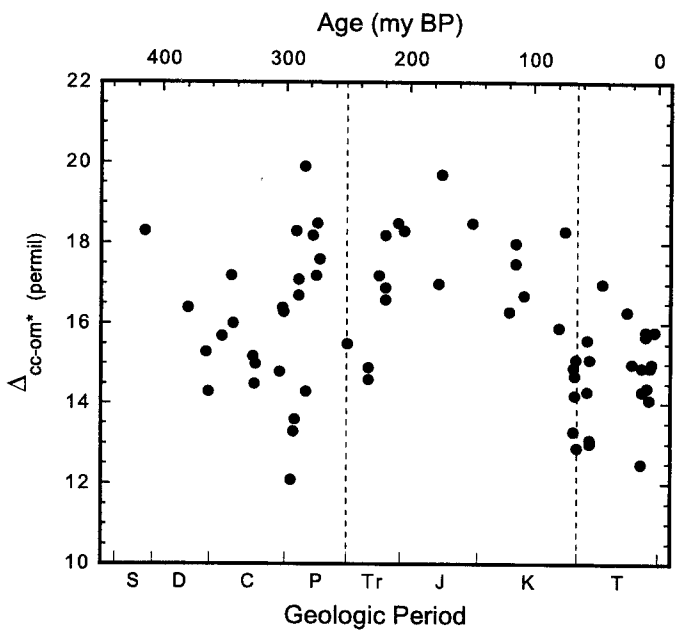

Fig. 9. The difference between carbon isotope compositions of pedogenic carbonates and proxy organic matter values ($\Delta_{cc\text{-}om^*}$). Larger differences theoretically represent the effects of higher atmospheric CO_2.

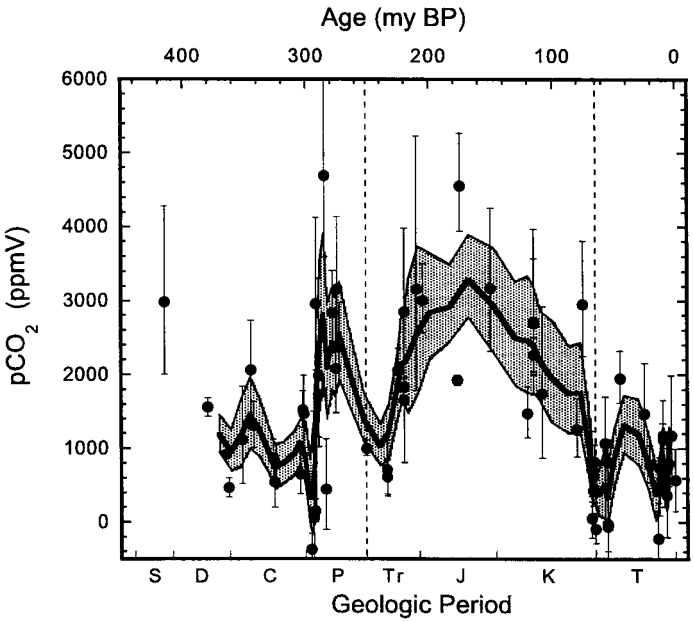

Fig. 10. Results of the pCO_2 paleobarometer. The solid circles represent our best estimates of pCO_2 levels for each group of data (tables 2, 3, and 4) using average isotopic compositions of pedogenic carbonates. The heavy curve is a 5 point weighted running average of these results. The uncertainty bars represent duplicate calculations using the average isotopic composition of pedogenic carbonates ± 1 standard deviation holding other variables constant. The area between the 5 point weighted running averages of the 'error' bars is lined.

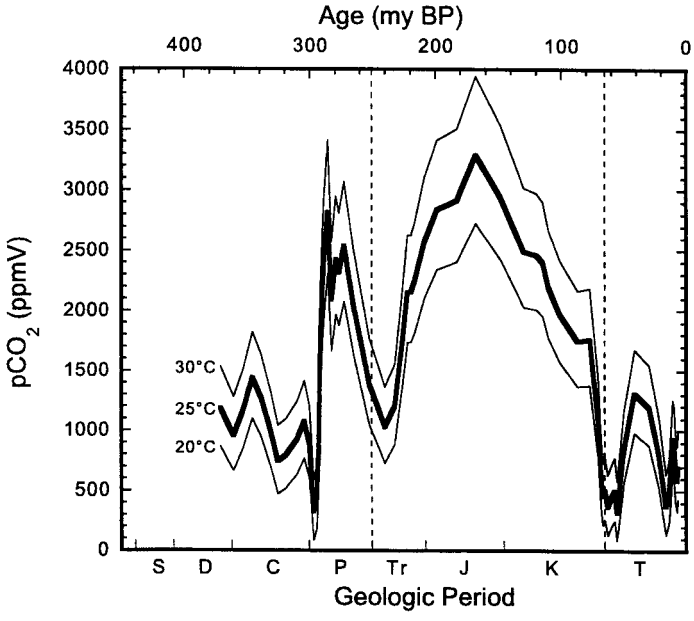

Fig. 11. Calculated pCO_2 levels assuming different soil paleotemperatures. The three curves each represent the 5 point weighted running averages as in figure 10.

paleosol morphology (Tabor and Montañez, 1999) and may signify the end of Late Paleozoic glaciation (López-Gamundí, 1997; Veevers and Powell, 1987). The details of this interpretation, including the magnitude and timing of the change in atmospheric CO_2, are strongly dependent on the $\delta^{13}C$ of the atmosphere and correlation between terrestrial and marine sedimentary records. The $\delta^{13}C$ of the atmosphere, which is based on the marine $\delta^{13}C$ record of Veizer and others (1999), has a high uncertainty in this interval. This transition may prove to be an important analog to changes in the modern atmospheric chemistry.

Mesozoic.–Results indicate that carbon dioxide levels increased from approx 1000 ppmV at the beginning of the Triassic, to approx 3000 ppmV by the end of the period, a level maintained through the Jurassic. The Cretaceous period began with high pCO_2 levels that declined throughout the period, culminating in levels similar to the modern condition prior to the Cretaceous-Tertiary transition. Analyses from three continents (four formations) of Maastrichtian age consistently indicate pCO_2 levels were at their lowest since the Late Paleozoic. It is intriguing that an accelerated pCO_2 decrease in the Late Cretaceous generally coincides with the proliferation of angiosperms (Ligard and Crane, 1990). Did the spread and diversification of angiosperms contribute to lowering of CO_2 levels (Volk, 1989), or were angiosperms opportunistic and spread as a result of lowered CO_2 levels? The downward trend in pCO_2 could be related to the tremendous quantities of carbon deposited in Cretaceous marine shales, chalks, and coals.

Cenozoic.–Cenozoic pCO_2 levels did not achieve the highest concentrations of the earlier eras. A possible oscillation during the Cenozoic is suggested, albeit by sparse data, with higher levels of CO_2 in the Eocene and Oligocene. Increased pCO_2, beginning at the Paleocene/Eocene boundary was inferred by Rea and others (1990) from a synthesis of geological evidence such as increased tectonism and sea-floor hydrothermal activity. Paleobotanical evidence indicates that the Eocene was the warmest period of the Cenozoic (Wolfe, 1978). More data from Cenozoic paleosols should elucidate the role of atmospheric carbon dioxide in the evolution of Cenozoic climates.

The emergence of C4 ecosystems during the Miocene (Quade and Cerling, 1995) has been hypothesized to be the result of a reduction in atmospheric pCO_2 (Cerling and others, 1997). A case for such a reduction in pCO_2 at approx 10 my can be made from the results listed in table 2, though this conclusion is tentative due to uncertainties of the same magnitude as the change in pCO_2 listed. Other periods of low pCO_2 (specifically parts of the Maastrichtian and Paleocene epochs) have occurred previous to the Miocene, with little evidence for expansion of biomass using the C4 photosynthetic pathway.

Comparison to other records.–A comparison of results with other methods is illustrated in figure 12. These other approaches allow an independent evaluation of our results. Each of these methods offer different temporal resolutions and optimal sensitivities at differing CO_2 levels. The model presented here has greater sensitivity at relatively high CO_2 levels but poor resolution below atmospheric pCO_2 concentrations of about 1000 ppmV.

Overall, the various results depicted in figure 11 show an overall decrease in pCO_2 through the Phanerozoic, similar to the results of this study. A high degree of similarity is evident between our results and the Berner (1994) GEOCARB II model, except in the Permian. It should be noted that the use of Phanerozoic surface ocean carbonates $\delta^{13}C$ links our results, to some degree, with other methods utilizing this database. Other than the low pCO_2 result obtained in the Jurassic, the results of Yapp and Poths (1992, 1996) are qualitatively similar to those reported here. Results from the models of Worsley and others (1994) are broadly in line with the results presented here, showing an overall decreasing trend though the Phanerozoic. Estimates of pCO_2 from marine organic matter and carbonates (Pagani, Freeman, and Arthur, 1999; Pagani, Arthur, and

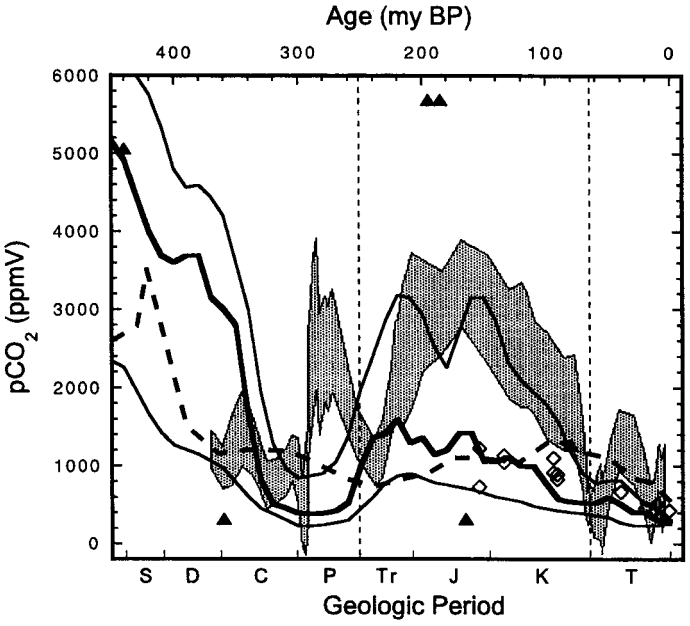

Fig. 12. Comparison of the fossil soil paleobarometer with other CO_2 estimates. The stippled area represents the results of this study. The GEOCARB II model (Berner, 1994) is depicted with soild lines, including the margins of uncertainty. The dashed line is the result from Worsley and others (1994). Solid triangles represent Yapp and Poths (1996) soil goethite based results. Open circles are from Freeman and Hayes (1992) pCO_2 estimates.

Freeman, 1999; Freeman and Hayes, 1992) are consistent with our results over the last 100 my but diverge sharply in the Early Cretaceous and Jurassic periods.

CONCLUSIONS

Paleo-pCO_2 levels have been calculated from a database of carbon isotope compositions of pedogenic carbonates. Proxy records for the isotopic compositions of the atmosphere and soil OM were calculated from a published compilation (Veizer and others, 1999) of surface ocean carbonate data. Individual calculations were used to calculate the trend of atmospheric carbon dioxide levels for the last 400 my. Results indicate that CO_2 concentrations varied significantly during the Paleozoic and Mesozoic eras, with less variation in the Cenozoic. Fossil soils bearing pedogenic carbonate are common in the rock record, such that improvements to this record of pCO_2 should be forthcoming with more analyses.

ACKNOWLEDGMENTS

Thanks to Pete Peterson, Christine Turner, Tim Demko, Steve Hasiotis, Brian Currie, Dan Chure, Aaron Handzlik, Eric Kvale, Bruce MacFadden, Alan Rigby, and NPS personnel for assistance in the field. Ben Passey provided assistance in the laboratory. Thanks to the SIRFER facility personel. Funding was provided by the National Science Foundation and the National Park Service.

References

Andrews, J. E., Tandon, S. K., and Dennis, P. F., 1995, Concentration of carbon dioxide in the Late Cretaceous atmosphere: Journal of the Geological Society, London, v. 152, p. 1–3.

Balesdent, J., and Mariotti, A., 1996, Measurement of soil organic matter turnover using ^{13}C natural abundance, *in* Boutton, T. W., and Yamasaki, S., editors, Mass spectrometry of soils: New York, Marcel Dekker, Inc., p. 83–111.

Barnola, J. M., Raynaud, D., Korotkevich, Y. S., and Lorius, C., 1987, Vostok ice core provides 160,000-year record of atmospheric CO_2: Nature (London), v. 329, p. 408–414.

Baver, L. D., Gardner, W. H., and Gardner, W. R., 1972, Soil physics: New York, John Wiley, 498 p.

Bemis, B. E., Spero, H. J., Bijima, J., and Lea, D. W., 1998, Reevaluation of the oxygen isotopic composition of planktonic foraminifera; experimental results and revised paleotemperature equations: Paleoceanography, v. 13, p. 150–160.

Berner, R. A., 1997, The rise of plants and their effects on weathering and atmospheric CO_2: Science, v. 276, p. 544–545.

—— 1994, GEOCARB II: a revised model of atmospheric CO_2 over Phanerozoic time: American Journal of Science, v. 294, p. 56–91.

—— 1992, Weathering, plants, and the long-term carbon cycle: Geochimica et Cosmochimica Acta, v. 56, p. 3225–3231.

—— 1991, A model for atmospheric CO_2 over Phanerozoic time: American Journal of Science, v. 291, p. 339–376.

Berner, R. A., Lasaga, A. C., and Garrels, R. M., 1983, The carbonate-silicate geochemical cycle and its effect on atmospheric carbon dioxide over the past 100 million years: American Journal of Science, v. 283, p. 641–683.

Bocherens, H., Friis, E. M., Mariotti, A., and Pederson, K. R., 1993, Carbon isotopic abundances in Mesozoic and Cenozoic fossil plants: Palaeoecological implications: Lethaia, v. 26, p. 347–358.

Bowring, S. A., Erwin, D. H., Jin, Y. G., Martin, M. W., Davidek, K., and Wang, W., 1998, U/Pb Zircon geochronology and tempo of the end-Permian mass extinction: Science, v. 280, p. 1039–1045.

Brook, G. A., Folkoff, M. E., and Box, E. O., 1983, A world model of soil carbon dioxide: Earth Surface Landforms, v. 8, p. 79–88.

Buchmann, N., Brooks, R. J., Flanagan, L. B., and Ehleringer, J. R., 1998, Carbon isotope discrimination of terrestrial ecosystems, *in* Griffiths, H., editor, Stable Isotopes: Integration of biological, ecological and geochemical processes: Oxford, United Kingdom, BIOS Scientific Publications, p. 203–221.

Buol, S. W., Hole, F. D., and McCracken, R. J., 1989, Soil genesis and classification: Ames, Iowa State University press, 446 p.

Cerling, T. E., 1999, Stable carbon isotopes in palaeosol carbonates, *in* Thiry, M., Simm-Coinçon, editors, Palaeoweathering, palaeosurfaces and related continental deposits: Oxford, Blackwells, p. 43–60.

—— 1992, Use of carbon isotopes in paleosols as an indicator of the $p(CO_2)$ of the paleo-atmosphere: Global Biogeochemical Cycles, v. 6, p. 307–314.

—— 1991, Carbon dioxide in the atmosphere: evidence from Cenozoic and Mesozoic paleosols: American Journal of Science, v. 291, p. 377–400.

—— 1984, The stable isotopic composition of modern soil carbonate and its relationship to climate: Earth and Planetary Science Letters, v. 71, p. 229–240.

Cerling, T. E., Ehleringer, J. R., and Harris, J. M., 1998, Carbon dioxide starvation, the development of C_4 ecosystems, and mammalian evolution: Philosophical transactions of the Royal Society of London, v. 353, p. 159–171.

Cerling, T. E., Harris, J. M., MacFadden, B. J., Leakey, M. G., Quade, J., Eisenmann, V., and Ehleringer, J., 1997, Global change through the Miocene/Pliocene boundary: Nature, v. 389, p. 153–158.

Cerling, T. E., and Quade, J., 1993, Stable carbon and oxygen isotopes in soil carbonates, *in* Swart, P. K., Lohmann, Kyger C., McKenzie, Judith A., Savin, S., editors, Climate change in continental isotopic records: Washington, D.C., American Geophysical Union, p. 217–231.

Cerling, T. E., Quade, J., Ambrose, S. H., and Sikes, N. E., 1991, Fossil soils, grasses, and carbon isotopes from Fort Ternan, Kenya: grassland or woodland?: Journal of Human Evolution, v. 21, p. 295–306.

Cerling, T. E., Solomon, D. K., Quade, J., and Bowman, J. R., 1991, On the isotopic composition of carbon in soil carbon dioxide: Geochimica et Cosmochimica Acta, v. 55, p. 3403–3406.

Davidson, G. R., 1995, The stable isotopic composition and measurement of carbon in soil CO_2: Geochimica et Cosmochimica Acta, v. 59, p. 2485–2489.

Degens, E. T., 1969, Biogeochemistry of stable carbon isotopes, *in* Eglinton, G., and Murphy, M. T. J., editors, Organic geochemistry; methods and results: New York, Springer-Verlag, p. 304–329.

Driese, S. G., Mora, C. I., Cotter, E., and Foreman, J. L., 1992, Paleopedolodgy and stable isotope chemistry of Late Silurian vertic paleosols, Bloomsburg Formation, central Pennsylvania: Journal of Sedimentary Petrology, v. 62, p. 825–841.

Farquhar, G. D., Ehleringer, J. R., and Hubic, K. T., 1989, Carbon isotope discrimination and photosynthesis: Annual Review of Plant Physiology and Plant Molecular Biology, v. 40, p. 503–537.

Freeman, K. H., and Hayes, J. M., 1992, Fractionation of carbon isotopes by phytoplankton and estimates of ancient CO_2 levels: Global Biogeochemical Cycles, v. 6, p. 185–198.

Friedli, H., Lötscher, H., Oeschger, H., Siegenthaler, U., and Stauffer, B., 1986, Ice core record of the 13C/12C ratio of atmospheric CO_2 in the past two centuries: Nature, v. 324, p. 237–238.

Ghosh, P., Bhattacharya, S. K., and Jani, R. A., 1995, Palaeoclimate and palaeovegetation in central India during the Upper Cretaceous based on stable isotope composition of the palaeosol carbonates: Palaeogeography, Palaeoclimatology, Palaeoecology, v. 114, p. 285–296.

Gile, L. H., Peterson, F. F., and Grossman, R. B., 1966, Morphological and genetic sequences of carbonate accumulation in desert soils: Soil Science, v. 101, p. 347–360.
Harland, W. B., Armstrong, R. L., Cox, A. V., Craig, L. E., Smith, A. G., and Smith, D. G., 1990, A geologic time scale 1989: New York, Cambridge University Press, 263 p.
IAEA/WMO, 1998, The GNIP database, Release 2. Global network for isotopes in precipitation: International Atomic Energy Agency.
Jenny, H., 1941, Factors of soil formation; a system of quantitative pedology: New York, McGraw-Hill, 281 p.
Jones, T. P., 1994, ^{13}C enriched Lower Carboniferous fossil plants from Donegal, Ireland: carbon isotope constraints on taphonomy, diagenesis and palaeoenvironment: Review of Palaeobotany and Palynology, v. 81, p. 53–64.
Keeling, C. D., 1994, Global historical CO_2 emissions, *in* Boden, T. A., Kaiser, D. P., Sepanski, R. J., Stoss, F. W., and Logsdon, F. W., editors, Trends '93; a compendium of data on global change: Springfield, Virginia, American Geological Institute, p. 501–504.
Keeling, C. D., Whorf, T. P., 1998, Atmospheric CO2 concentrations–Mauna Loa Observatory, Hawaii, 1958–1997, http://cdiac.esd.ornl.gov/ftp/ndp001/maunaloa.co2.
Kenny, R., and Neet, K. E., 1993, Upper Pennsylvanian-Permian (Naco Group) paleosols (north-central Arizona): field and isotopic evidence: Geoderma, v. 58, p. 131–148.
Kirkham, D., and Powers, W. L., 1972, Advanced soil physics: New York, Wiley-Interscience.
Koch, P. L., Zachos, J. C., and Dettman, D. L., 1995, Stable isotope stratigraphy and paleoclimatology of the Paleogene Bighorn Basin (Wyoming, USA): Palaeogeography, Palaeoclimatology, Palaeoecology, v. 115, p. 61–89.
Kürschner, W. M., Van der Burgh, J., Visscher, H., and Dilcher, D. L., 1996, Oak leaves as biosensors of late Neogene and early Pleistocene paleoatmospheric CO_2 concentrations: Marine Micropaleontology, v. 27, p. 299–312.
Lidgard, S., and Crane, P. R., 1990, Angiosperm diversification and Cretaceous floristic trends; a comparison of palynofloras and leaf macrofloras: Paleobiology, v. 16, p. 77–93.
López-Gamuní, O. R., 1997, Glacial-postglacial transition in the Late Paleozoic basins of southern South America, *in* Martini, I. P., editor, Late glacial and postglacial environmental changes: Quaternary, Caroniferous-Permian, and Proterozoic: New York, Oxford University Press, p. 147–168.
Lynch-Stieglitz, J., Stocker, T. F., Broecker, W. S., and Fairbanks, R. G., 1995, The influence of air-sea exchange on the isotopic composition of oceanic carbon: Observations and modeling: Global Biogeochemical Cycles, v. 9, p. 653–665.
Mack, G. H., Cole, D. R., Giordano, T. H., Schaal, W. C., and Barcelos, J. H., 1991, Paleoclimatic controls on stable oxygen and carbon isotopes in caliche of the Abo Formation (Permian), South-central New Mexico, U.S.A.: Journal of Sedimentary Geology, v. 61, p. 458–472.
Mack, G. H., James, W. C., and Monger, H. C., 1993, Classification of paleosols: Geological Society of America Bulletin, v. 105, p. 129–136.
Magaritz, M., 1989, ^{13}C mimima follow extinction events: A clue to faunal radiation: Geology, v. 17, p. 337–340.
McCrea, J. M., 1950, On the isotopic chemistry of carbonates and a paleotemperature scale: Journal of Chemical Physics, v. 18, p. 849–857.
McElwain, J. C., and Chaloner, W. G., 1996, The fossil cuticle as a skeletal record of environmental change: Palaios, v. 11, p. 376–388.
Mora, C. I., and Driese, S. G., 1993, A steep, mid- to late Paleozoic decline in atmospheric CO_2: evidence from the soil carbonate CO_2 paleobarometer: Chemical Geology, v. 107, p. 217–219.
Mora, C. I., Driese, S. G., and Colarusso, L. A., 1996, Middle to Late Paleozoic atmospheric CO_2 levels from soil carbonate and organic matter: Science, v. 271, p. 1105–1107.
Mora, C. I., Driese, S. G., and Seager, P. G., 1991, Carbon dioxide in the Paleozoic atmosphere: Evidence from carbon-isotope compositions of pedogenic carbonate: Geology, v. 19, p. 1017–1020.
Muchez, P., Peeters, C., Keppens, E., and Viaene, W. A., 1993, Stable isotopic composition of paleosols in the Lower Viséan of eastern Belgium: evidence of evaporation and soil-gas CO_2: Chemical Geology, v. 106, p. 389–396.
Nadelhofer, K. J., and Fry, B., 1988, Controls on natural nitrogen-15 and carbon-13 abundances in forest soil organic matter: Soil Science Society of America Journal, v. 52, p. 1633–1640.
Pagani, M., Arthur, M. A., and Freeman, K. H., 1999, Miocene evolution of atmospheric carbon dioxide: Paleoceanography, v. 14, p. 273–292.
Pagani, M., Freeman, K. H., and Arthur, M. A., 1999, Late Miocene atmospheric CO_2 concentrations and the expansion of C_4 grasses: Science, v. 285, p. 876–879.
Pearce, E. A., and Smith, C. G., 1984, The world weather guide: London, Hutchinson, 480 p.
Popp, B. N., Takigiku, R., Hayes, J. M., Louda, J. W., and Baker, E. W., 1989, The post-Paleozoic chronology and mechanism of 13C depletion in primary marine organic matter: American Journal of Science, v. 289, p. 436–454.
Purvis, K., and Wright, V. P., 1991, Calcretes related to phreatophytic vegetation from the Middle Triassic Otter Sandstone of south west England: Sedimentology, v. 38, p. 539–551.
Quade, J., and Cerling, T. E., 1995, Expansion of C_4 grasses in the late Miocene of northern Pakistan: evidence from stable isotopes in paleosols: Palaeogeography, Palaeoclimatology, Palaeoecology, v. 115, p. 91–116.
Quade, J., Cerling, T. E., and Bowman, J. R., 1989, Systematic variations in the carbon and oxygen isotopic composition of pedogenic carbonate along elevation transects in the southern Great Basin, United States; with Suppl. Data 89-10: Geological Society of America Bulletin, v. 101, p. 464–475.

Quade, J., Solounias, N., and Cerling, T. E., 1994, Stable isotopic evidence from paleosol carbonates and fossil teeth in Greece for forest or woodlands over the past 11 Ma: Palaeogeography, Palaeoclimatology, Palaeoecology, v. 108, p. 41–53.
Rasbury, E. T., Hanson, G. N., Meyers, W. J., Holt, W. E., Goldstein, R. H., and Saller, A. H., 1998, U-Pb dates of paleosols: Constraints on late Paleozoic cycle durations and boundary ages: Geology, v. 26, p. 403–406.
Rea, D. K., Zachos, J. C., Owen, R. M., and Gingerich, P. D., 1990, Global change at the Paleocene-Eocene boundary: climatic and evolutionary consequences of tectonic events: Palaeogeography, Palaeoclimatology, Palaeoecology, v. 79, p. 117–128.
Retallack, G. J., 1988, Field recognition of paleosols, *in* Reinhardt, J., and Sigleo, W. R., editors, Paleosols and weathering through geologic time; principles and applications: Reston, VA, Geological Society of America, p. 1–20.
—— 1990, Soils of the past; An introduction to paleopedology: Boston, Unwin Hyman, 520 p.
Romanek, C. S., Grossman, E. L., and Morse, J. W., 1992, Carbon isotopic fractionation in synthetic aragonite and calcite: Effects of temperature and preciptation rate: Geochimica et Cosmochimica Acta, v. 56, p. 419–430.
Shackleton, N. J., Hall, M. A., Line, J., and Shuxi, C., 1983, Carbon isotope data in core V19–30 confirm reduced carbon dioxide concentration in the ice age atmosphere: Nature, v. 306, p. 319–322.
Singh, J. S., and Gupta, S. R., 1977, Plant decomposition and soil respiration in terrestrial ecosystems: Botanical Review, v. 43, p. 449–528.
Sinha, A., Stott, L. D., 1994, New atmospheric pCO_2 estimates from paleosols during the late Paleocene/early Eocene global warming interval: Global and Planetary Change, v. 9, p. 297–307.
Soil Survey Staff, 1983, Soil Taxonomy: A basic system of soil classification for making and interpreting soil surveys: Malabar, Florida, Robert E. Erieger Publishing Co., Inc., 754 p.
Solomon, D. K., and Cerling, T. E., 1987, The annual carbon dioxide cycle in a montane soil: observations, modeling, and implications for weathering: Water Resources Research, v. 23, p. 2257–2265.
Stewart, W. N., 1983, Paleobotany and the evolution of plants: Cambridge, Cambridge University Press, 450 p.
Suchecki, R. K., Hubert, F. F., and Birney de Wet, C. C., 1988, Isotopic imprint of climate and hydrogeochemistry on terrestrial strata of the Triassic-Jurassic Hartford and Fundy rift basins: Journal of Sedimentary Petrology, v. 58, p. 801–811.
Tabor, N. J., Montañez, I. P., 1999, Early Permian atmospheric pCO_2 reconstructed from paleosol carbonate: Implications for Late Paleozoic deglaciation: Bathurst meeting, 11th University of Cambridge.
Tajika, E., Matsui, T., 1992, Evolution of terrestrial proto-CO_2 atmosphere coupled with thermal history of the earth: Earth and Planetary Science Letters, v. 113, p. 251–266.
Veevers, J. J., and Powell, C. McA., 1987, Late Paleozoic glacial episodes in Gondwanaland reflected in transgressive-regressive depositional sequences in Euramerica: Geological Society of America Bulletin, v. 98, p. 475–487.
Veizer, J., Ala, D., Azmy, K., Bruckschen, P., Buhl, D., Bruhn, F., Carden, G. A. F., Diener, A., Ebneth, S., Godderis, Y., Jasper, T., Korte, C., Pawellek, F., Podlaha, O. G., and Strauss, H., 1999, $^{87}Sr/^{86}Sr$, $\delta^{13}C$ and $\delta^{18}O$ evolution of Phanerozoic seawater: Chemical Geology, v. 161, p. 59–88.
Volk, T., 1989, Rise of the angiosperms as a factor in long-term climatic cooling: Geology, v. 17, p. 107–110.
Wahlen, M., Mastroianni, D., Deck, B., and Bacastow, R., 1993, Reconstruction of atmospheric CO_2 and delta $^{13}CO_2$ over the last 1000 years from air of the GISP2 ice core: Eos, Transactions, American Geophysical Union, v. 74, p. 78.
White, J. W. C., Ciais, P., Figge, R. A., Kenny, R., and Markgraf, V., 1994, A high-resolution record of atmospheric CO_2 content from carbon isotopes in peat: Nature, v. 367, p. 153–156.
Wolfe, J. A., 1978, A paleobotanical interpretation of Tertiary climates in the Northern Hemisphere: American Scientist, v. 66, p. 694–703.
Worsley, T. R., Moore, T. L., Fraticelli, C. M., and Scotese, C. R., 1994, Phanerozoic CO_2 levels and global temperatures inferred from changing paleogeography, *in* Klein, G. D., editor, Pangea: Paleoclimate, tectonics, and sedimentation during accretion, zenith, and breakup of a supercontinent: Boulder, Geological Society of America Special Paper 288, p. 57–73.
Yapp, C. J., and Poths, H., 1992, Ancient atmospheric CO_2 pressures inferred from natural goethites: Nature (London), v. 355, p. 342–344.
—— 1996, Carbon isotopes in continental weathering environments and variations in ancient atmospheric CO_2 pressure: Earth and Planetary Science Letters, v. 137, p. 71–82.